Pergamon

Cement and Concrete Research, Vol. 27, No. 12, pp. 1829–1839, 1997

0008-8846/97 $17.00 + .00

PII S0008-8846(97)00179-8

IMPROVING BRICK-TO-MORTAR BOND STRENGTH BY THE ADDITION OF CARBON FIBERS TO THE MORTAR

M. Zhu and D.D.L. Chung[1]
Composite Materials Research Laboratory, State University of New York at Buffalo, Buffalo, NY 14260-4400

(Refereed)
(Received March 19, 1997; in final form September 4, 1997)

ABSTRACT

The addition of short carbon fibers in the optimum amount of 0.5% of the cement weight to mortar increased the brick-to-mortar bond strength by 150% under tension and 110% under shear when the gap between the adjoining bricks was fixed, and by 50% under tension and 44% under shear when this gap was allowed to freely decrease due to the weight of the brick above the joint. This effect is attributed to a decrease of the drying shrinkage by the fiber addition. The drying shrinkage decrease was particularly large at 2 to 24 h of curing. At 24 h, the shrinkage was decreased by 50% by the addition of fibers in the amount of 0.5% of the cement weight. Fibers in excess of the optimum amount gave less bond strengthening due to increased porosity in the mortar.

Introduction

The durability of brick constructions is limited by the bond strength between brick and mortar (1). The bond strength can be affected by the mortar strength, mortar shrinkage, brick strength, joint thickness, interface morphology, and chemical bond (1–4). The drying shrinkage of the mortar weakens the brick-to-mortar bond because of the fact that the mortar shrinks as it cures in a brick-to-brick joint, whereas the adjoining bricks do not shrink. This situation is even more serious in the head joints (i.e., vertical joints) of the masonry wall and in the tuck pointing of old brick constructions, because the gaps between the bricks are fixed.

Carbon fiber-reinforced mortar provides an avenue for increasing the brick-mortar bonding strength, because the carbon fibers can increase the mortar strength and decrease the drying shrinkage as well (5). It was reported that, by adding 0.35 vol.% short carbon fibers to new mortar, the shear bond strength of the old-new mortar joint was increased by up to 89% (6). It is important to investigate the usefulness of carbon fiber-reinforced mortar in the masonry field for the purpose of obtaining brick-mortar bonds of improved strength.

In this work, it was found that the addition of carbon fibers (optimum amount = 0.5% by weight of cement) to the mortar increased the brick-to-mortar bond strength. The fractional

[1]To whom correspondence should be addressed.

TABLE 1
Mix Properties of Various Types of Mortar

Mortars	Fiber		Water/ cement ratio	Sand/ cement ratio	Meth/ cement (%)	SF/ cement ratio	WR/ cement (%)	Lime/ cement ratio
	% by wt. of cement	vol. %						
Plain mortar	0	0	0.475	1	0.4	0.15	2	—
Mortars	0.25	0.175	0.475	1	0.4	0.15	2	—
with	0.5	0.35	0.475	1	0.4	0.15	2	—
fibers	1.0	0.70	0.475	1	0.4	0.15	3	—
	2.0	1.4	0.475	1	0.4	0.15	3	—
ASTM C270 mortars	—	—	0.75–1.5	2.25–3	—	—	—	0.25–2.5

Note: Meth = methylcellulose; SF = silica fume; WR = water reducing agent.

increase was 150% under tension and 110% under shear when the gap between the adjoining bricks was fixed, and was 50% under tension and 44% under shear when this gap was allowed to freely decrease due to the weight of the brick above the joint. Fiber contents beyond the optimum gave lower strengths due to increased porosity in the mortar.

Experimental

Materials and Sample Preparation

Table 1 describes the mix proportions of the mortars used in this work. They are different from the standard proportions for mortars for unit masonry as described in ASTM C270. In ASTM C270, it is required that one part of Portland cement be mixed with ¼–2½ parts of lime and 2¼–3 parts of sand to form different types of mortar that meet different property requirements, such as workability, water retentivity, bond strength, durability extensibility, and compressive strength. Moreover, economy is a driving force for the use of lime and sand. It was reported (7,8) that the lower the proportions of lime and sand, the greater the compressive strength and the bonding strength. In this work, to achieve a high bond strength, we eliminated the lime portion of the mortar and fixed the sand/cement ratio at 1:1. As required by dispersing the carbon fibers (4), methylcellulose and silica fume were added; they were used whether the fibers were present or not in order to investigate the effect of the fiber addition alone. In addition, silica fume modifies the workability, mechanical properties, microstructure, and durability of concrete (10) and improves the flexural strength and toughness of carbon fiber-reinforced concrete (11).

The carbon fibers used (Table 2) were short, unsized, and based on isotropic pitch. They were provided as Carboflex by Ashland Petroleum Co. (Ashland, Ky) and were used in amounts of 0, 0.25, 0.5, 1, and 2% of the cement weight (equivalent to 0, 0.175, 0.35, 0.70, and 1.4 volume% respectively). The cement was Portland cement, Type I, from Lafarge Corporation (Southfield, MI). The sand was natural sand (100% passing a 2.36-mm sieve,

TABLE 2
Properties of Carbon Fibers

Nominal length	5 mm
Filament diameter	10 μm
Tensile strength	690 MPa
Tensile modulus	48 GPa
Elongation at break	1.4%
Electrical resistivity	3.0×10^{-3} Ω·cm
Specific gravity	1.6 g cm^{-3}
Carbon content	98 wt. %

99.91% SiO_2). The particle size analysis of the sand is shown in Figure 1 of Ref. 12. Table 3 describes the various raw materials used. The silica fume was used in the amount of 0.15 of the weight of the cement. Methylcellulose was used in the amount of 0.4% of the cement weight. The defoamer (Colloids 1010), always used along with methylcellulose, was in the amount of 0.13 volume%. The water reducing agent powder was TAMOL SN (Rohm and Haas), which contained 93–96% sodium salt of a condensed naphthalenesulfonic acid. The water reducing agent/cement ratio was 2% for fiber contents of 0, 0.25, and 0.5% of the weight of the cement, and was 3% when the fiber content was 1% or 2% of the weight of the cement. In general, the slump of carbon fiber-reinforced cement tends to decrease with increasing carbon fiber content. The water/cement ratio was 0.475 at all fiber contents.

The bricks used were of two types, namely red 3-hole bricks (202 × 90 × 56 mm) and red paving bricks (197 × 89 × 57 mm). They were extruded, wire cut, clay units that comply with the requirements of ASTM C216 and ASTM C902. The 3-hole bricks were used for tensile debonding testing, such that the joining surface was the smooth edge surface of the brick. The paving bricks (with no hole) were used for shear debonding testing, such that the joining surface was the rough large surface of the brick.

Methylcellulose was dissolved in water, and then the fibers and defoamer were added and stirred by hand for about 2 min. Then sand, cement, water, and water-reducing agent were successively added and mixed in a Hobart mixer with a flat beater for 5 min.

The Portland cement in the mortar requires water to initiate and continue the hydration for setting and hardening. Thus, the availability of water for hydration is of prime importance. Because the bricks may absorb water from the mortar, thereby decreasing the bond strength

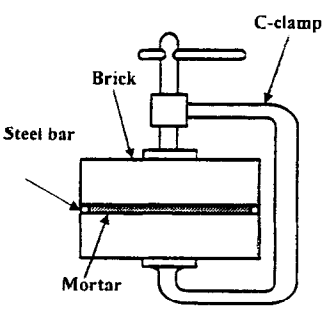

FIG. 1.
Joint configuration for the case of the gap being fixed.

TABLE 3
List of Raw Materials

Material	Source
Portland cement Type I	Lafarge Corporation (Southfield, MI)
TAMOL SN Sodium salt of a condensed naphthalenesulfonic acid (93–96%) Water (51–54%)	Rohm and Haas Company (Philadelphia, PA)
Methocel, A15-LV Methylcellulose	Dow Chemical Corporation (Midland, MI)
Colloids 1010 Defoamer	Colloids Inc. (Marietta, GA)
Silica fume	Elkem Materials Inc. (Pittsburgh, PA)
Carboflex Carbon fibers	Ashland Petroleum Company (Ashland, KY)

(13), all the bricks in this work were immersed in water for about 3 h. Then they were wiped dry and the mortar was applied on them. By water immersion, the possibility of water absorption by the bricks was reduced.

The gap between the adjoining brick surfaces were either kept fixed during curing (by placing two parallel 11-mm diameter steel bars between the bricks and near the edges of the bricks and using a C-clamp to keep the gap between the bricks constant, as shown in Fig. 1) or allowed to decrease freely during curing due to the weight of the brick above the joint (by not having any steel bar between the bricks). In the first case, the steel bars were placed on the lower brick and the mortar was placed to fill the space between the bars. Then the upper brick was placed on top of the bars and a C-clamp was used to hold everything together. Thus, the gap between the bricks was kept constant during the curing of the mortar. The excess mortar was squeezed out from the gap and was scraped off. Special fixtures were attached to the steel bars during the sample preparation in order to make sure that the bars were in the right position and were parallel to the edge of the brick. In the latter case, the same procedure was followed, except that the C-clamp was not used and the two steel bars were carefully withdrawn from the joint prior to curing. The pressure due to the brick above the joint was 2.1 kPa for the tensile debonding test and was 1.5 kPa for the shear debonding test. The former case is relevant to the joining of the vertical edges of side-by-side bricks in a brick wall and to the tuck pointing (repair) of brick structures. The latter case is relevant to the joining of the horizontal surfaces of bricks on top of one another in a brick wall.

No vibrator was used to consolidate the mortar. Curing of the mortar took place in air, with the temperature at 20–25°C and the relative humidity at 55–65%.

Testing

Debonding tests were conducted under tension (Fig. 2) and shear (Fig. 3) using a Sintech 2/D screw-type mechanical testing system at 7 days of curing. Under tension, the force was

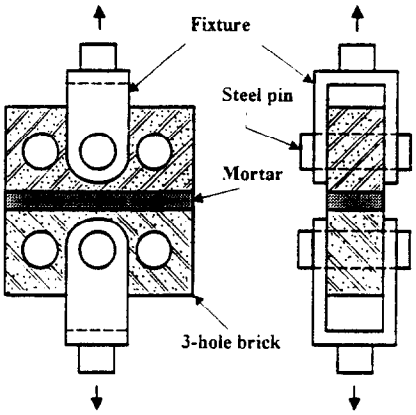

FIG. 2.
Sample configuration for tensile debonding testing.

applied in a direction perpendicular to the joint. Under shear, the force was applied in a direction parallel to the joint. Six samples of each fiber content were tested for each configuration. In both cases, debonding occurred mostly at the brick-mortar interface. Table 4 gives the bond strength obtained for various fiber contents. At any fiber content, the bond strength, whether tensile or shear, was much higher when the gap was not fixed than when the gap was fixed, as expected. Whether under tension or shear, and whether the gap was fixed or not, the bond strength increased with increasing fiber content up to 0.5% of the cement weight and then decreased with further increase in the fiber content.

Figure 4 shows optical photographs of mortars with fibers in amounts of 0, 0.5, and 2% of the cement weight. The needle-like objects are fibers that happened to lie in the plane of the photographs. The bright regions are sand; the dark regions are pores, which are mostly smaller than the sand particles. The porosity increased with increasing fiber content. The ASTM method C29/C29M-91a was used to measure the porosity and density of mortars with different fiber contents. As shown in Table 5, the porosity increased with increasing fiber content. Because the fiber addition increased the viscosity of the mortar mixture and no vibrator was used, the chance that air voids generated during mixing would remain in the

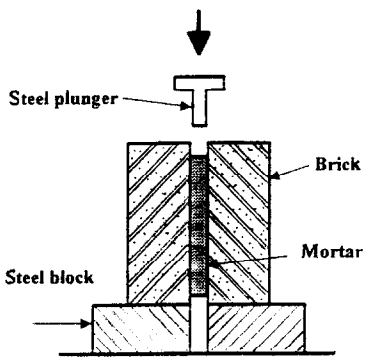

FIG. 3.
Sample configuration for shear debonding testing.

TABLE 4
Brick/Brick Joint Strength (kPa)

Fiber/cement ratio (%)	Tensile*		Shear*	
	Gap not fixed	Gap fixed	Gap not fixed	Gap fixed
0	348.5 (±5%)	39.4 (±5%)	437.3 (±4%)	126.5 (±5%)
0.25	406.1 (±4%)	61.4 (±5%)	506.6 (±4%)	178.4 (±6%)
0.5	524.4 (±3%)	97.3 (±4%)	631.7 (±5%)	267.5 (±3%)
1.0	285.6 (±6%)	49.7 (±6%)	429.1 (±5%)	224.0 (±6%)
2.0	174.1 (±5%)	35.8 (±8%)	454.3 (±6%)	217.7 (±7%)

*Average of 6 tests

mortar after curing increased with increasing fiber content. This is believed to be the main reason why the mortar porosity increased with the fiber content.

Figure 5 shows optical photographs of the cross-sectional view of the brick-mortar interface. Figure 5a and b, both without fibers, show that, in the presence of pressure during curing (i.e., the case of the gap being not fixed), the mortar was able to fill the irregularities in the brick surface, but, in the absence of pressure (i.e., the case of the gap being fixed), the mortar was not able to fill the irregularities in the brick surface, thus leaving voids at these irregularities. This is mainly why the bond strength is higher in the case of the gap being not fixed. Another reason is that the shrinkage stress at the brick-mortar interface is less when the gap is not fixed. Figures 5b, c, and d, all cases of the gap being not fixed, show that the pores became more abundant as the fiber content increased, and some pores even occupied irregularities in the brick surface (Fig. 5d). That the bond strength decreased with increasing porosity (air content) has been previously reported (13).

The drying shrinkage strain during curing was measured for curing ages from 2 to 24 h using a Perkin-Elmer thermal mechanical analyzer (TMA7) (Fig. 6) and for curing ages from 1 to 14 days in accordance with ASTM C490–83a (Fig. 7). In the former method, the 5-mm diameter cylindrical specimen was 12 mm long along the cylindrical axis (direction of length measurement), and the length change measurement accuracy was ± 0.00001 mm (± 0.01 μm). In the latter method, the 25.4 mm × 25.4 mm rectangular specimen was 286 mm long in the direction of length measurement and the length-change measurement accuracy was ±0.0025 mm. Although the two methods used quite different specimen sizes (12 mm vs. 286 mm), the high sensitivity of TMA7 (± 0.01 μm vs. ± 2.5 μm) more than made up for the size disadvantage. More accurate drying shrinkage measurement results were obtained from the first method (± 0.24 μm at the 286-mm sample size vs. ± 2.5 μm at the 286-mm sample size). The effect of fiber addition on the drying shrinkage was much more in Figure 6 than Figure 7. The combination (addition of the strains) of Figures 6 and 7 gives Figure 8, which shows the complete picture from 2 h to 14 days. Both Figures 6 and 8 show that the fiber addition reduced the drying shrinkage most severely at low fiber contents, i.e., 0.25 and 0.5% of the cement weight. Further increase in the fiber content gave only incremental effects.

Discussion

The addition of carbon fibers to mortar in the amount of only 0.5% of the cement weight greatly increases the brick-to-mortar bond strength. The fractional strength (tension or shear)

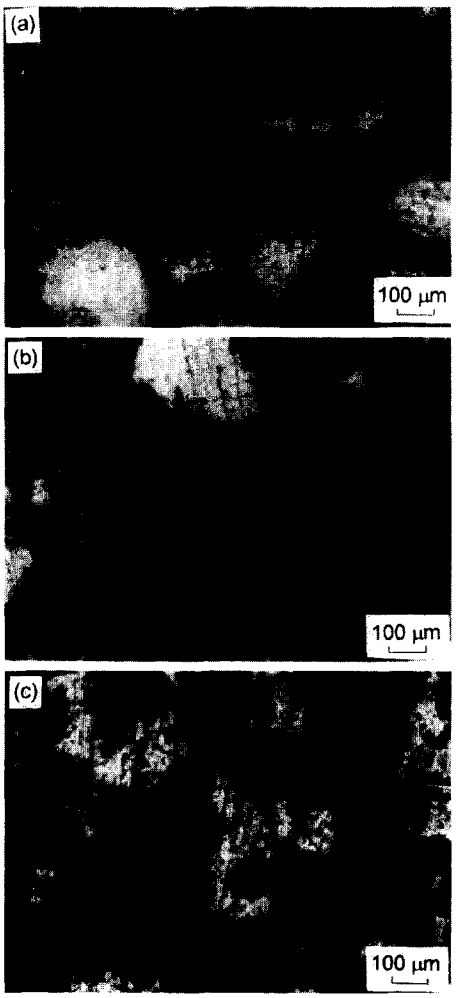

FIG. 4.
Optical photographs of the mortars with carbon fibers in amounts of (*a*) 0%, (*b*) 0.5%, and (*c*) 2% of the cement weight.

increase is larger when the gap between the adjoining bricks is fixed than when the gap is not fixed. The fractional strength increase is similar under tension and shear. This bond strengthening is practically useful. When considering the high labor cost of building or repairing a brick structure, the increased mortar cost due to the fiber addition is incremental in the overall cost. When considering the mortar price alone, the fiber addition in the amount of 0.5% of the cement weight (together with the addition of methylcellulose, silica fume and defoamer) results in a mortar price increase of approximately 30%.

The fiber addition decreases the drying shrinkage and increases the porosity of the mortar. The decrease in the drying shrinkage helps to increase the bond strength, whereas the increase in the porosity decreases the bond strength. Thus the overall effect is that the highest bond strength occurs at an intermediate fiber content of 0.5% of the cement weight.

TABLE 5
Porosity and Density of Mortars

Fiber/cement ratio (%)	Porosity (%)	Density (g/cm^3)
0	1.5	1.937
0.25	5.8	1.824
0.5	10.1	1.741
1.0	24.8	1.458
2.0	29.5	1.371

Drying shrinkage is conventionally measured from a curing age of 1 day onward, in accordance with ASTM C490–83a. Neglecting the shrinkage at curing ages less than 1 day (24 h) is a pity, especially when practical brick-to-mortar bonding is considered. It was reported that it takes about 2 h for Portland cement to start hardening (14,15). This means that after 2 h, the cement is not in a plastic state and shrinkage stress can be generated. Thus, it is important to measure the drying shrinkage at curing age from 2 to 24 h. By measuring the drying shrinkage in this period, in addition to that from 1 to 14 days, we found that the

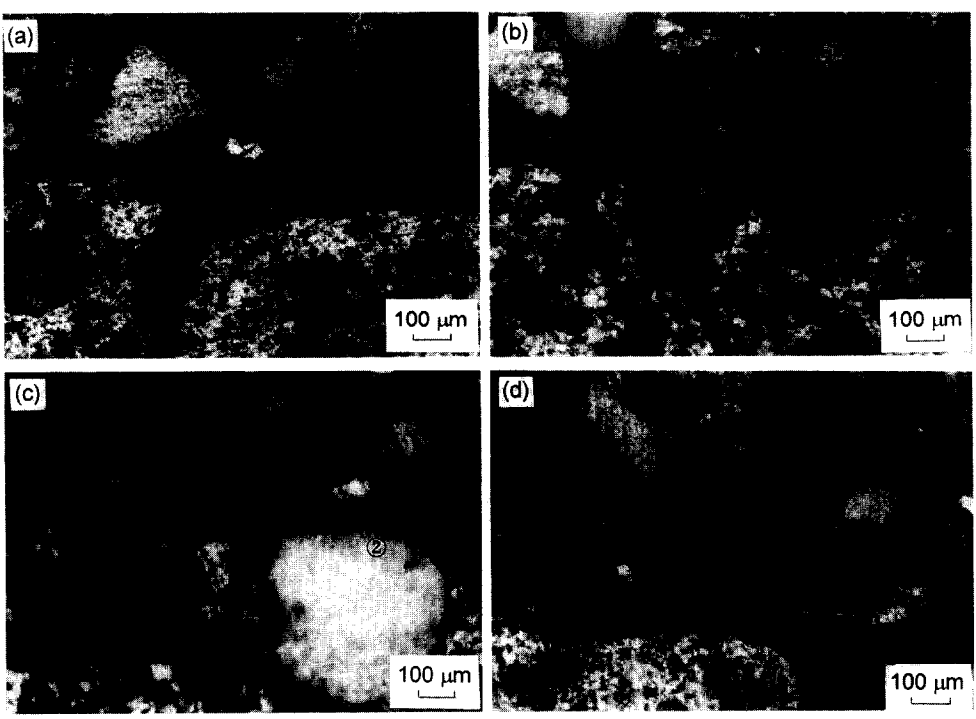

FIG. 5.
Optical photographs of the cross-sectional view of the brick-mortar interface. The brick is labeled 2, below the black outline; the mortar is labeled 1, above the black outline in each photograph. (*a*) no fibers, fixed gap, (*b*) no fibers, gap not fixed, (*c*) fibers in the amount of 0.5% of the cement weight, gap not fixed, and (*d*) fibers in the amount of 2% of the cement weight, gap not fixed.

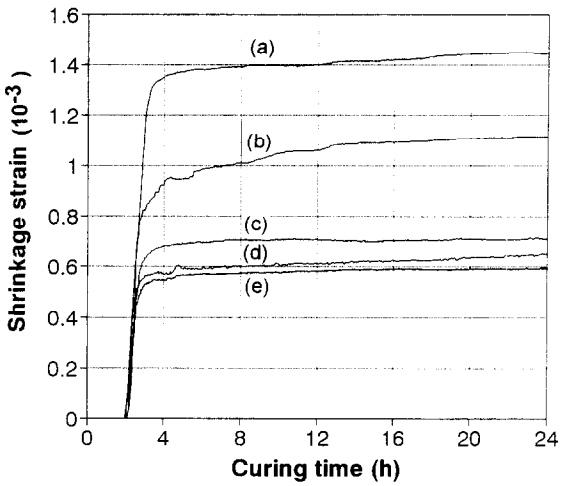

FIG. 6.

Drying shrinkage strain vs. curing time from 2 to 24 h. Fibers in amounts of (*a*) 0%, (*b*) 0.25%, (*c*) 0.5%, (*d*) 1.0%, and (*e*) 2.0% of the cement weight.

magnitude of the shrinkage strain from 2 to 24 h is large, and the effect of the fiber addition on the shrinkage is much more significant in the period from 2 to 24 h than the period from 1 to 14 days. At 24 h, the shrinkage strain is decreased by 50% by the addition of carbon fibers in the amount of 0.5% of the cement weight. If the shrinkage measurement starts at 1 day, the shrinkage strain at 14 days is decreased by 16% by the addition of fibers in the same amount. Besides the difference in the starting time for measuring the drying shrinkage, the fact that the shrinkage of mortar is more than concrete should be considered. Therefore, the

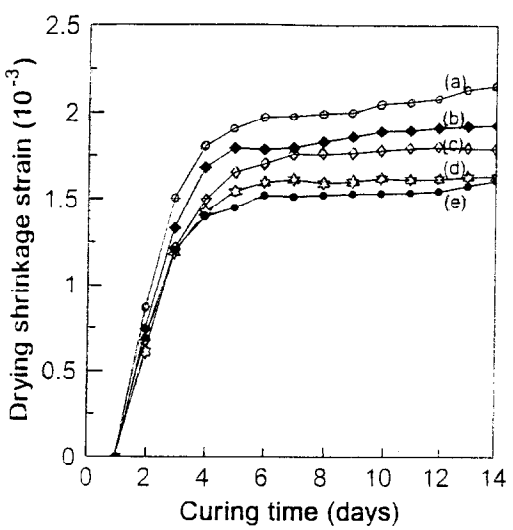

FIG. 7.

Drying shrinkage strain vs. curing time from 1 to 14 days. Fibers in amounts of (*a*) 0%, (*b*) 0.25%, (*c*) 0.5%, (*d*) 1.0%, and (*e*) 2.0% of the cement weight.

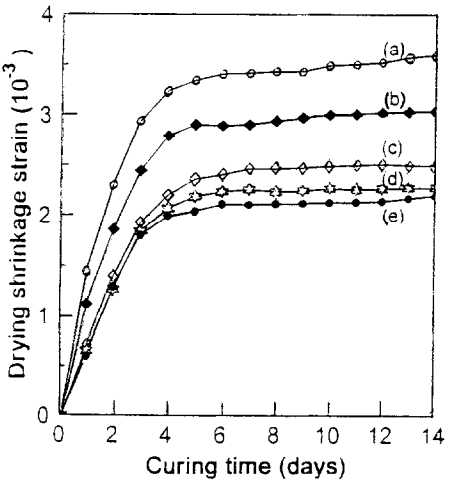

FIG. 8.
Drying shrinkage strain vs. curing time from 2 h to 14 days. Fibers in amounts of (*a*) 0%, (*b*) 0.25%, (*c*) 0.5%, (*d*) 1.0%, and (*e*) 2.0% of the cement weight.

fiber addition has more significant influence on the drying shrinkage in this work (mortar) than in previous work (concrete) (9,12). The shrinkage strain data at 24 h or less show that the fibers' effectiveness for decreasing the shrinkage is larger at fiber contents less than 0.5% of the cement weight.

Because of the size of the sample holder, the sample was small (5 mm diameter, 12 mm long) for the drying shrinkage test from 2 to 24 h. Due to the fact that the average length of the fibers is 5 mm, it may be of concern that the fiber orientation in the tested samples does not represent the actual fiber orientation in the practical situation, and that this may affect the accuracy of the shrinkage data. However, an examination of the curves of shrinkage strain vs. curing time in Figure 6 shows that the slope of the curve from 2 h to 1 day (by using small samples) and that of the curve from 1 day to 2 days (by using standard size samples) closely match for every value of fiber content. Therefore, it is believed that the fiber orientation under our test conditions will not significantly affect the accuracy of the drying shrinkage data. The drying shrinkage from 2 to 24 h is a substantial contribution to the overall shrinkage and should not be neglected.

ASTM E519 describes the standard test method for determining the shear bond strength of masonry assemblages or the shear bond strength of the mortar-to-brick joints. This method requires a large specimen size (1.2 m square), a large testing machine, and large fixtures, so its usage is limited. Small-scale specimens are of interest. Hendry (16) pointed out that a three-brick specimen was used by a number of investigators, as it can be tested without any special equipment. The test results were found to correlate satisfactorily with the ASTM E519 method. In the three-brick method, the three bricks are joined by two mortar layers. During the test, the two bricks sandwiching the center brick are supported at the bottom and the load is applied on the top of the center brick. The maximum load divided by the bonded surface is considered the shear bond strength. However, because the load is applied on the center brick rather than exactly on the joint plane, a bending moment results on the joint interface. Moreover, the weight of the center brick adds to the bending moment. Therefore,

this method does not provide "pure" shear testing. In this work, we developed a two-brick method (Fig. 3), in which two bricks are joined by a mortar layer. The load is directly applied on the joint layer, so the bending moment and the center brick's weight effect are not present. Therefore, our method is closer to "pure" shear testing. Furthermore, our sample configuration is simpler than that of the three-brick method. Due to the low stress (Table 4) needed for debonding, the induced splitting tensile stress perpendicular to the plane of the joint is negligible.

The brick-to-mortar bond strength values (Table 4) obtained for the case of the gap being not fixed are of the same order of magnitude as those previously reported using similar methods (1,17). No previous report has been made for the case of the fixed gap. Because a fixed gap exists in vertical joints in a masonry wall and in tuck pointing old brick constructions, and the associated bond strength is much lower than the case of the gap being not fixed (Table 4), much more attention should be paid to the case of the fixed gap.

Conclusion

Carbon fibers decreased the drying shrinkage of mortar. The drying shrinkage from 2 to 24 h is important, though it is usually neglected. Due to the drying shrinkage reduction, brick/brick joint strength was increased by adding carbon fibers to the mortar. The highest joint strength was attained at a fiber content of 0.5% by weight of cement. The joint strength was much higher for the joint with gap not fixed than with gap fixed.

References

1. E. Jung, Brick and Block Masonry, J.W. de Courcy (ed.), pp. 182–193, Elsevier Applied Science, 1988.
2. C.J.W.P. Groot, Brick and Block Masonry, J.W. de Courcy (ed.), pp. 175–181, Elsevier Applied Science, 1988.
3. A.W. Hendry, Structural Brickwork, pp. 29–31, Wiley, 1981.
4. S.J. Lawrence and H.T. Cao, Brick and Block Masonry, J.W. de Courcy (ed.), pp. 194–204, Elsevier Applied Science, Philadephia, 1988.
5. P.-W. Chen and D.D.L. Chung, Compos. 24, 33 (1993).
6. P.-W. Chen, X. Fu, and D.D.L. Chung, Cem. Concr. Res. 25, 491 (1995).
7. M. Mehlmann and B. Oppermann, Brick and Block Masonry, J.W. de Courcy (ed.), pp. 139–149, Elsevier Applied Science, 1988.
8. J.M. Melander and J.T. Conway, Masonry: Design and Construction, Problems and Repair, ASTM STP 1180, ASTM, Philadelphia, 1993.
9. P.-W. Chen and D.D.L. Chung, J. Elect. Mater. 24, 47 (1995).
10. K.H. Khayat and P.C. Aitcin, Proc. 4th Int. Conf. Fly Ash, Silica Fume, Slag and Natural Pozzolans in Concrete, 835–872.
11. P.-W. Chen, X. Fu, and D.D.L. Chung, ACI Mater. J. 94, 147 (1997).
12. P.-W. Chen and D.D.L. Chung, Smart Mater. Struct. 2, 22 (1993).
13. B.T. Wright, R.D. Wilkins, and G.W. John, Masonry: Design and Construction, Problems and Repair, ASTM STP 1180, pp. 197–210, ASTM, Philadelphia, 1993.
14. A.M. Neville, Properties of Concrete, 3rd ed., Pitman Publishing Limited, London, 1981.
15. S. Giertz-Hedstorm, Proc. 2nd Int. Symp. Chem. Cem. 505–534 (1938).
16. A.W. Hendry, Structural Brickwork, pp. 33–52, Wiley, New York, 1981.
17. A.W. Isberner, Designing Engineering and Constructing with Masonry Products, F.B. Johnson (ed.), pp. 42–49, Gulf Publishing Company, Texas, 1969.